**Atmospheric
Chemistry
and Physics**
Open Access
Discussions

A mechanism for biologically-induced iodine emissions from sea-ice

A. Saiz-Lopez[1], C. S. Blaszczak-Boxe[2,3], and L. J. Carpenter[4]

[1]Atmospheric Chemistry and Climate Group, Institute of Physical Chemistry Rocasolano, CSIC, Madrid, Spain
[2]Department of Physical, Environmental and Computer Sciences Medgar Evers College-City University of New York, Brooklyn, NY 11235, USA
[3]CUNY Graduate Center, Chemistry Division, Earth and Environmental Science, Division, Manhattan, NY 10016, USA
[4]Wolfson Atmospheric Chemistry Laboratories, Department of Chemistry, University of York, Heslington, York YO10 5DD, UK

Correspondence to: A. Saiz-Lopez (a.saiz@csic.es)

Discussion Paper | Discussion Paper | Discussion Paper | Discussion Paper |

ACPD

15, 10257–10297, 2015

A mechanism for biologically-induced iodine emissions from sea-ice

A. Saiz-Lopez et al.

Title Page

Abstract	Introduction
Conclusions	References
Tables	Figures

|◄ | ►|

◄ | ►

Back | Close

Full Screen / Esc

Printer-friendly Version

Interactive Discussion

Abstract

Ground- and satellite-based measurements have reported high concentrations of iodine monoxide (IO) in coastal Antarctica. The sources of such a large iodine burden in the coastal Antarctic atmosphere remain unknown. We propose a mechanism for iodine release from sea-ice based on the premise that micro-algae are the primary source of iodine emissions in this environment. The emissions are triggered by the biological production of iodide (I^-) and hypoiodous acid (HOI) from micro-algae (contained within and underneath sea-ice) and their diffusion through sea-ice brine channels, to accumulate in the quasi-liquid layer (QLL) on the surface of sea-ice. Prior to reaching the QLL, the diffusion timescale of iodine within sea-ice is depth-dependent. The QLL is also a vital component of the proposed mechanism as it enhances the chemical kinetics of iodine-related reactions, which allows for the efficient release of iodine to the polar boundary layer. We suggest iodine is released to the atmosphere via 3 possible pathways: (1) emitted from the QLL and then transported throughout snow atop sea-ice, to be released to the atmosphere, (2) released directly from the QLL to the atmosphere in regions of sea-ice that are not covered with snowpack; or (3) emitted to the atmosphere directly through fractures in the sea-ice pack. To investigate the proposed biology-ice-atmosphere coupling at coastal Antarctica we use a multiphase model that incorporates the transport of iodine species, via diffusion, at variable depths, within brine channels of sea-ice. Model simulations were conducted to interpret observations of elevated springtime IO in the coastal Antarctic, around the Weddell Sea. The results show that the levels of inorganic iodine (i.e., I_2, IBr, ICl) released from sea-ice through this mechanism could account for the observed IO concentrations during this timeframe. The model results also indicate that iodine may trigger the catalytic release of bromine from sea-ice through phase equilibration of IBr. We propose that this mechanism may also result in the emission of iodocarbons from the sea-ice to the polar atmosphere. Considering the extent of sea-ice around the Antarctic continent, we sug-

gest that the resulting high levels of iodine may have widespread impacts on catalytic ozone destruction and aerosol formation in the Antarctic lower troposphere.

1 Introduction

Over the past two decades, evidence has accumulated for the role of atmospheric iodine in the catalytic destruction of tropospheric ozone (e.g., Chameides and Davis, 1980; Solomon et al., 1994; Vogt et al., 1999; McFiggans et al., 2000; Calvert and Lindberg, 2004a; Saiz-Lopez et al., 2007a, 2012, 2014; Read et al., 2008; Sommariva and von Glasow, 2012; Carpenter et al., 2013). In the mid-latitude marine boundary layer (MBL) iodine decreases the HO_x ratio (i.e., $[HO_2]/[OH]$) via the reaction of IO and HO_2 to form HOI, which then photolyzes efficiently to OH, whereas NO oxidation to NO_2 by IO increases the NO_x ratio (i.e., $[NO_2]/[NO]$) (e.g., Bloss et al., 2005). In other words, iodine atoms released from photolysis react rapidly with O_3 to form IO; rapid reactions of IO with HO_2 and NO_2, followed by photochemical breakdown, results in the regeneration of atomic iodine without forming O_3 and therefore in catalytic O_3 destruction.

Considerable attention has been given to the role of iodine oxides in the formation of ultra-fine aerosol (i.e., 3–10 nm diameter) and its potential to contribute to cloud condensation nuclei (CCN) formation (O'Dowd et al., 1998, 2002; Hoffmann et al., 2001; Jimenez et al., 2003; Saiz-Lopez and Plane, 2004; McFiggans et al., 2004; Burkholder et al., 2004; Sellegri et al., 2005; Saunders and Plane, 2005, 2006; Saiz-Lopez et al., 2006; Pechtl et al., 2006; Atkinson et al., 2012; Gomez Martin et al., 2013; Galvez et al., 2013). Iodine has also been suggested to impact the depletion of gaseous elemental mercury (Hg°) by oxidation to reactive gaseous mercury (Hg^{II}) (Calvert and Lindberg, 2004b; Saiz-Lopez et al., 2008; Wang et al., 2014).

IO is formed following photolysis of photo-labile reactive iodine precursors and the subsequent reaction of I atoms with atmospheric O_3. In the polar boundary layer IO has been detected in coastal Antarctica by ground – (Friess et al., 2001; Saiz-Lopez et al.,

2007a; Atkinson et al., 2012) and satellite-based instrumentation (Saiz-Lopez et al., 2008; Schönhardt et al., 2008, 2012), and also by ground-based techniques in the Arctic boundary layer (Mahajan et al., 2010). These studies have shown iodine to be very abundant (e.g., up to 20 pptv during Antarctic springtime) and widespread around coastal Antarctica, which have been proposed to significantly impact the chemistry and vertical distribution of O_3, HO_x, NO_x, and Hg in the coastal Antarctic marine boundary layer (Saiz-Lopez et al., 2008).

In the polar regions the source of reactive inorganic bromine and chlorine includes heterogeneous reactions involving sea-salt bromide on sea-ice, snowpack, or marine aerosol surfaces (e.g., Saiz-Lopez and von Glasow, 2012 and references therein). These heterogeneous reactions take part in an autocatalytic cycle that destroys ozone while preserving atomic halogen radicals. However, these mechanisms do not result in significant iodine release to the gas phase due to the comparatively much smaller content of iodide in sea-salt. Over the continental Antarctic snowpack two mechanisms have been proposed to explain the observed large levels of IO: (i) direct release of reactive iodine from snowpack (Frieß et al., 2010), and (ii) aerosol deposition and subsequent recycling on snowpack (Saiz-Lopez et al., 2008). However, in sea-ice areas around coastal Antarctica, iodocarbons (i.e. CH_3I, CH_2ICl, CH_2I_2, CH_2IBr) levels have been found to be insufficient to account for the high concentrations of gas phase iodine due to their relatively long photolytic lifetimes, as compared to inorganic precursors, and small concentrations (Atkinson et al., 2012; Granfors et al., 2015). Therefore, although the presence of high levels of reactive iodine in the coastal Antarctic boundary layer has already been evidenced, the sources and mechanisms of iodine release over sea-ice covered areas in coastal Antarctica still remain unclear. In this study a hypothesis for iodine release from sea-ice is presented. The suggested coupling between biology, sea-ice and overlying atmosphere is investigated using a multiphase chemical model.

2 Physical context of the polar sea ice environment

Sea-ice is one of the most extreme and largest ecosystems in the polar ocean (Eicken, 1992a, 2003; Brierley and Thomas, 2002; Arrigo and Thomas, 2004). Sea-ice is not completely solid and can, at times, be comprised of a system of brine channels that provide a habitat, characterized by low temperatures ($253 \leq T/K \leq 271$), high salinity (35–200 psu), high pH (up to 11), and low irradiances (1 µmol photons $m^{-2} s^{-1}$) at the sea-ice–water interface (Eicken, 1992b; Gleitz et al., 1995; Kirst and Wiencke, 1995).

Seawater starts to freeze as temperatures drop below $-1.86\,°C$ (271.30 K) since it generally contains about 35 g of dissolved salts (e.g., sodium, calcium sulphate, magnesium, chloride, and potassium). Ice begins to form and rise to the surface, forming frazil ice in various physical shapes and dimensions. Thereafter, loosely aggregated pancakes (ice discs) form by the motion of wind and water to consolidate ice crystals. These pancake ice features propagate in both the lateral and vertical direction as time progresses, eventually forming packed ice, which is permeable to microscopic transport and impermeable to macroscopic transport – especially macroscopic transport of brine channel fluid. The vast majority of Antarctic sea-ice is comprised of frazil and platelet ice, compared to 80 % of columnar ice in the Arctic. This is primarily due to the fact that Antarctic sea-ice is formed with more turbulent water compared to much calmer conditions experienced in the Arctic (Margesin et al., 2007; Eicken, 2003a).

Salts, ions, and air in the water are concentrated into inclusions of pockets and channels or released into the water below the sea-ice as they cannot be incorporated into ice crystals during the formation of sea-ice. Hence, sea-ice is a solid matrix penetrated by a labyrinth of channels and pores that contain highly concentrated brine and air bubbles. Brine channels are defined as vertically-elongated tubular systems containing fluid, with diameters of less than a few millimeters to several centimeters and exhibit a vertical extent up to 50 cm at coastal Antarctica (Thomas and Dieckmann, 2003). They are also the main habitat for all micro-organisms in sea-ice (Brierley and Thomas, 2002; Deming, 2002; Lizotte, 2003; Moch and Thomas, 2005; Mock and Junge, 2007).

Salt concentration and brine volume are directly proportional to temperature (Eicken, 2003b; Weissenberger et al., 1992; Krembs et al., 2000); therefore, as temperature increases, brine volume increases and salt concentration decreases. Hence, colder ice contains brine channels with highly salty brines and overall fewer, smaller and less interconnected channels than warmer ice. Gradients exist in temperature, brine salinity, and brine volume since ice at the air–ice interface is usually colder than ice in contact with underlying water. A suite of protists and zooplankton have been recorded to live in sea-ice (Horner, 1986; Palmisano and Garrison, 1993; Lizotte, 2003; Schnack-Schiel, 2003; Werner, 2006). Among the autotrophs, the most studied are diatoms. All discovered organisms within sea-ice have plastic physiologies to cope with these dynamic changes (dominated by temperature and salinity changes) in physical and chemical conditions of their environment.

As sea-ice forms, micro-algae get caught between the ice crystals or simply stick to them as crystals rise through the water when it freezes in the fall. Diatoms become trapped within brine channels during the formation of consolidated ice. Pennate diatoms, along with other micro-algae (e.g., dinoflagellates, flagellates) are the most conspicuous organisms in sea-ice (Brierley and Thomas, 2002; Thomas and Dieckmann, 2002; Lizotte, 2003). These micrometer-sized algae, with their main light harvesting pigment, fucoxanthin, can attain such concentrations in sea-ice that they discolor the ice visibly brown. The time for acclimation to new conditions is not very long since daylight hours continue to decrease as winter approaches. Nevertheless, diatoms, especially at the ice–water interface, are often able to photo-acclimate rapidly and can accumulate to high biomass even before the winter begins (Gleitz and Thomas, 1993). Sea-ice diatoms are very efficient at optimizing solar irradiance and are able to grow at low irradiance levels – below 1 µmol photons $m^{-2} s^{-1}$ (Mock and Graddinger, 1999). Light levels are minimal during polar winter due to short days/complete darkness and snow cover atop sea-ice, which acts as a very efficient reflector of solar irradiance (Eicken, 2003b).

A mechanism for biologically-induced iodine emissions from sea-ice

A. Saiz-Lopez et al.

Title Page

Abstract	Introduction
Conclusions	References
Tables	Figures

|◄ | ►|

◄ | ►

Back | Close

Full Screen / Esc

Printer-friendly Version

Interactive Discussion

Maximum growth rates for polar diatoms are 0.25–0.75 divisions per day – i.e. 2- to 3-fold slower than growth rates at temperatures above 10 °C (Sommer, 1989). Many of these diatoms are psychrophilic and cannot live at temperatures above ca. 15 °C, indicative of the presence of specific molecular adaptations that enable these diatoms to grow under freezing temperatures. Only recently, functional genomics were applied to various/specific diatoms to begin to uncover the molecular basis of growth and, thus, adaptation to polar conditions (Mock and Valtentin, 2004; Mock et al., 2006).

Most notably, Hill and Manley (2009) investigated the release of reactive iodine from diatoms. Via an in situ incubation assay, they measured the iodination of phenol red to detect the release of reactive iodine, primarily hypoiodous acid (HOI) from a putative extracellular bromoperoxidase of marine diatoms. Six of 11 species showed significant release compared to controls. Polar diatoms were especially active, releasing 0.02–2.7 µmol HOI [mg total chlorophyll]$^{-1}$ h^{-1}, at 100 µmol L^{-1} iodide concentration. Therefore, micro-algae are a major source of iodine, complementing Kupper et al. (1998)'s study of enhanced iodine uptake in macro-algae. Hill and Manley (2009) find that the release of (not only iodine) but also bromine species can account for a significant amount of their emissions needed to simulate polar tropospheric ozone depletion events.

3   Model description

In order to study the link between polar marine micro-algae iodine emissions and the potential for iodine release from sea-ice, we developed the multiphase chemical model (Condensed-Phase-to-Air Transfer Model, CON-AIR). This model incorporates the multi-component aspect of sea-ice (e.g., ice, quasi-liquid layer (QLL), brine channels, and micro-algae), interfaced with overlying atmospheric boundary layer chemistry. It is structured in three main components: (i) micro-algae emissions and transport through sea-ice brine channels, (ii) aqueous phase chemistry regime in the QLL; and (iii) gas phase chemistry scheme comprising photochemical, thermal and heterogeneous reactions.

A mechanism for biologically-induced iodine emissions from sea-ice

A. Saiz-Lopez et al.

Title Page

Abstract | Introduction

Conclusions | References

Tables | Figures

◀ | ▶

◀ | ▶

Back | Close

Full Screen / Esc

Printer-friendly Version

Interactive Discussion

3.1 Aqueous and gas phase chemistry in CON-AIR

The QLL is defined as a thin layer on the surface of sea-ice and ice crystals that comprise snowpack and sea-ice, where water molecules are not in a rigid solid structure, yet not in the random order of liquid (Petrenko and Whitworth, 1999). The aqueous phase component treats 14 species and comprises 25 condense phase reactions, representing iodine, bromine, and chlorine chemistry in the QLL. The gas phase chemistry includes 41 chemical species, 154 reactions representative of the standard O_3-NO_x-HO_x-S and halogen gas phase chemistry, along with a treatment of the halogen recycling on deliquesced airborne sea-salt aerosols. It also incorporates 12 processes of heterogeneous uptake and wet/dry deposition, and 38 photochemical reactions. The complete scheme of reactions in the QLL and the gas-phase employed in the model is summarized in the Supplement.

The exchange of halogen species between the liquid (QLL) and gas phase is treated via phase equilibration as well as deposition of gas phase molecules onto the sea-ice surface. For iodine species, this liquid-gas phase exchange depends upon the Henry's law constants of species including I_2, IBr and ICl. The gas phase equilibrating species, Henry's law solubility constants and temperature dependences are shown in Table 3 of the Supplement. The temperature dependence of the solubility of species is taken into account by including a diurnal variation of the typical temperature profile during springtime (i.e., $\sim 260 \leq T/K \leq \sim 270$) (Launiainen and Vihma, 1994).

3.2 Transport through sea-ice

Here, we consider only transport by diffusion, but this should be regarded as a lower-limit as transport is also governed by wind pumping, advection, thermal convection, and/or fluid transport. Fick's first law is used in steady-state diffusion – i.e., when the concentration within the diffusion volume does not change with respect to time ($J_{in} =$

J_{out}). In one (spatial) dimension,

$$J = -D\left(\frac{\partial \phi}{\partial x}\right), \tag{1}$$

where J is the diffusion flux (amount of substance/length^2 time^{-1}), D is the diffusion coefficient or diffusivity (length^2 time^{-1}), ϕ is the concentration (amount of substance length^{-3}), and x is the position (length). The range of diffusion coefficients used in this study range from 10^{-4} to 10^{-7} cm^2 s^{-1}, which are within the range of experimental data on diffusion of species in ice/snow (Shaw et al., 2011; Loose et al., 2011). We also use Fick's second law as the transport of iodine is in non-steady-state (or continually changing) since the concentration within the diffusion volume changes with respect to time.

$$\frac{\partial \phi}{\partial t} = D\left(\frac{\partial^2 \phi}{\partial x^2}\right), \tag{2}$$

where t is time.

Here, we solve Fick's second law via the limited-source-diffusion approximation and incorporate this solution into the model. Given the following boundary conditions:

$\phi(x,0) = 0$

$\int \phi(x,t)\mathrm{d}x = S$

$\phi(x,\infty) = 0,$

Where S is called the "dose," where $S(t) = \phi_o(4\mathrm{d}t/\pi)^{1/2}$, where ϕ_o is the initial concentration of iodine at the surface in the brine layer. The solution to Fick's Law under these conditions is: $\phi(x,t) = (S/(\pi \mathrm{d}t)^{1/2}) \times \exp(-x^2/4\mathrm{d}t)$. Therefore, at each time "t" "$\phi(x,t)$" was computed and then incorporated in Fick's First law at each specified time

"*t*" to compute *J* at each "*t*". We used this approximation to take into account the change in *J* as a function of time.

From late July/early August (transition from winter to spring) till late November/early December (transition from spring to summer), coastal Antarctic temperatures range from ~ 208 to 273 K (Schwerdtfeger, 1974; Veihelmann et al., 2001). This temperature regime encompasses both microscopic (gaseous diffusion through the snowpack/sea-ice crystal network, transport through water/brine veins) and macroscopic (transport of bulk brine through brine channels, water-vein transport) transport through sea-ice (see Sect. 2). This timeframe also coincides with the onset of the release of iodine and gradual decline of iodine release, from the start of summer onwards (Saiz Lopez et al., 2007a). The Antarctic Peninsula and the temperature regime of the Weddell Sea exhibit a temperature range from 256 to 270 K from the beginning till the end of spring (September to December). Via monthly averaged surface temperatures (Schwerdtfeger, 1974), the Antarctic Peninsula's east coast experiences temperatures 8 °C colder than the Antarctic Peninsula's west coast. During the timeframe of iodine release, the Antarctic Peninsula's west coast experiences temperatures at or above −5 °C, the lower-limit temperature demarcation, governing the "*rule of fives*" and thus lower-limit temperature boundary for macroscopic permeability (Golden et al., 1998). Prior to this study, it was shown that (unlike freshwater) sea-ice is a highly permeable medium for gases. It was shown that the migration of gases along grain boundaries (e.g., in brine channels) was 2 to 6 times as great as that at right angles to the principal axis of the grain boundaries (Gosink et al., 1976). At −15 °C, penetration rates of halogenated species were 30 and 60 cm h^{-1} for CO_2 (Gosink et al., 1976). The vertical migration is ~ twice as fast as horizontal migration at 15 °C; for semi-fresh pressure ridge ice, the migration rate was 60 cm h^{-1} at −15 °C. Gosink et al. (1976) produced estimated permeation constants of 10^{-7} and 10^{-5} cm^2 s^{-1} atm^{-1} for SF_6 at −15 °C and CO_2 at −7 °C.

Golden et al. (2007) showed that the columnar sea-ice permeability for liquids drop by approximately two orders of magnitude below a 5 % relative brine volume, which

corresponds to roughly −5 % for a bulk salinity of 5 (i.e., the "*rule of fives*"). It has long been observed (Weeks and Ackley, 1986) that columnar sea ice is effectively impermeable to brine transport for ice porosity less than 5 %, yet is permeable for ice porosity above 5 %. For a bulk salinity of 5 parts per thousand (ppt), the critical ice porosity ∼ 5 % corresponds to a critical temperature of −5 °C, via equations relating ice porosity to temperature and salinity (Thomas and Diekmann, 2003; Weeks and Ackley, 1986). Golden et al. (1998) discussed the rule of fives in terms where the critical ice porosity was identified with the critical probability in a continuum percolation model for a compressed powder (Kusy and Turner, 1971) – exhibiting microstructural characteristics qualitatively similar to sea-ice.

In the Arctic, strongly aligned columnar ice is the dominant textural type and accounts for ∼ 2/3 to 3/4 of the total ice volume. Dynamic growth conditions in the Antarctic limit the occurrence of columnar ice to the lower-most layers of the ice cover. While vertically oriented columnar crystals are common, horizontal alignment is observed only infrequently and generally both horizontal and vertical dimensions of columnar crystals in Antarctic sea-ice are smaller than their Arctic counterparts (Thomas and Diekmann, 2003). Therefore, the rule of fives has partial (at most 25 %) and minimal application for Arctic and Antarctic sea-ice, respectively, when solely considering ice microstructure. Antarctica's ice volume is comprised of frazil and platelet ice (Margesin et al., 2007; Eicken, 2003a; Thomas and Diekmann, 2003).

Brine entrapped in sea-ice will always be at or near freezing since any departure will either cause some of the water in the brine to freeze, or melting some of the surrounding ice. Thus, brine salinity is variable and can be determined based strictly on temperature-freezing point depression. Tucker et al. (1993), Heygster et al. (2009) and Ulaby et al. (1986) derived empirical formulas relating sea-ice temperature and brine salinity. These equations show that from −5 to −20 °C brine salinity ranges from ∼ 85 to 210 parts per thousand. Note, the eutectic temperature for NaCl is −21.2 °C; therefore, thin liquid films should exist well below zero with the porous component of sea-ice (apart from brine channels). Additional solutes will lower the freezing point of interfacial

thin films. Although (when compared to Arctic sea-ice) brine salinity is larger (overall) in Antarctica sea-ice; still, Arctic sea-ice brine salinity is predominantly over 5 parts per thousand (Vancoppenolle et al., 2009; Gleitz et al., 1995; Eicken, 2012; Arrigo and Sullivan, 1992). In addition (apart from past studies on sea-ice permeability/transport) (Gosink et al., 1976; Boxe, 2005), recent field observations of fluxes of trace gases also question the impermeability of sea-ice during winter (Heinesch et al., 2009; Miller et al., 2011) and spring (Semiletov et al., 2004; Delille, 2006; Zemmelink et al., 2006; Nomura et al., 2010a, b; Papakyriakou and Miller, 2011; Grannas et al., 2007).

Within the degree of uncertainty of a limited number of experiments on species transport in snow/ice, overall it appears that species in ice have some degree of appreciable mobility, which makes them to be impactful in polar tropospheric boundary layer chemistry (Boxe et al., 2003, 2005, 2006; Boxe and Saiz-Lopez, 2008; Grannas et al., 2007; Granfors et al., 2015). In other words, especially within the context of the suite of impurities contained in sea-ice/snowpack (with varying range of concentrations), macroscopic and microscopic transport is still possible outside of the physical parameters that govern the "*rule of fives*" as exemplified by the suite of field studies that have measured trace gases over the Arctic and Antarctic snowpack and sea-ice – over many decades – both in situ and remotely at much lower temperatures and a wide range of salinity levels. A given brine volume fraction can be attained by a variety of temperature and salinity combinations as shown by the Frankestein and Garner equations (Frankenstein and Garner, 1967). Pinpointing the critical conditions for impermeability is crucial. So – if the permeability of sea ice is so important, why have there not been extensive permeability measurements – like those done for porous materials? In most materials where permeability measurements are made, the matrix material does not react with the fluid passing through it. This is definitely not the case with sea ice, where slight differences between the temperature of the ice matrix and of temperature and salinity of brine can result in either the addition or the subtraction of ice from the matrix during the experimental procedure (Ono and Kasai, 1985; Saito and Ono, 1978; Maksym and Jeffries, 2000).

3.3 Aqueous phase scheme and QLL parameterizations

The initial concentrations of I^-, Br^- and Cl^- in the QLL are assumed to be that of the ions in seawater 1.3×10^{-7}, 8×10^{-4} and 0.545 M respectively (Wayne, 2000). This model assumes that all ions and molecular species reside in the QLL. In order to account for the concentration effect on the aqueous phase reaction rates the volume of the QLL needs to be calculated. Using a mean thickness for the Southern Ocean sea-ice and density of 50 cm and 0.91 g cm^{-3} (Thomas and Dieckmann, 2003), respectively, the total potential liquid content in a snow column of 1 cm^2 cross-sectional area of sea-ice is:

$$\text{total potential liquid content} = \frac{50 \, \text{cm} \times 0.91 \, \text{g cm}^{-3}}{1 \, \text{g cm}^{-3}} = 45.5 \, \text{cm}^3 \, \text{cm}^{-2} \tag{3}$$

The mean mass fraction of liquid water in ice between 265 and 250 K is 1×10^{-3} (Conklin and Bales, 1993). We calculate a mean QLL thickness $= 500$ µm by: sea-ice thickness $\times$ sea-ice cross-sectional area $\times$ mass fraction of liquid water $= 50$ cm $\times$ 1 cm^2 $\times$ $10^{-3} = 0.05$ cm^3; then, 0.05 cm^3/1 cm$^2 = 500$ µm. The QLL volume in sea-ice can now be calculated as:

$$\text{QLL volume} = 45.5 \, \text{cm}^3 \, \text{cm}^{-2} \times 1 \times 10^{-3} = 0.0455 \, \text{cm}^3 \, \text{cm}^{-2} \tag{4}$$

For an atmospheric boundary layer height of 400 m (40 000 cm) a volumetric factor is obtained:

$$\text{volumetric} = \frac{0.0455 \, \text{cm}^3 \, \text{cm}^{-2}}{40\,000 \, \text{cm}} = 1.14 \times 10^{-6} \left(\frac{\text{cm}^3 \, (\text{QLL})}{\text{cm}^3 \, (\text{atmosphere})} \right) \tag{5}$$

Therefore, the reaction rates are quantified incorporating the volumetric factor. We find that this enhancement in model concentrations and reaction rates due to the concentration effect of ions and molecular species in the QLL is necessary to provide ample

gas-phase concentrations. The rate constants for the QLL reactions are then expressed as:

$$k[1\,cm^3\,(atmosphere)]/[1.14 \times 10^{-6}\,(QLL)] \tag{6}$$

$$k[1\,cm^3\,(atmosphere)]^2/[1.14 \times 10^{-6}\,(QLL)]^2 \tag{7}$$

where k are the literature aqueous phase rate constants in units of $cm^3\,molecule^{-1}\,s^{-1}$ and $cm^6\,molecule^{-2}\,s^{-1}$, for second- and third-order rate constants, respectively.

The rate of transfer of species from the QLL to the gas phase is calculated using an approximation for the first-order rate constant, $k_t = 1.25 \times 10^{-5}\,s^{-1}$, previously suggested by (Gong et al., 1997; Michalowski et al., 2000):

$$k_{mix} = k_t \times \frac{40\,000\,cm^3\,(atmosphere)}{0.0455\,cm^3\,(QLL)} \tag{8}$$

However, the rate of transfer of species will depend on the concentration and Henry's law constants for solubility of the corresponding species. Hence, the complete expression for the phase equilibration of species from the QLL to the atmosphere is:

$$k_{(QLL \rightarrow Atmosphere)} = (k_{mix} \times [\text{species concentration}] \times \text{volumetric})/(H') \tag{9}$$

where H' is the dimensionless Henry's law constant. H' is accordingly defined as $H' = (HRT)$, where H is a species' Henry's law constant, R is the gas constant, $0.082058\,L\,atm\,K^{-1}\,mol^{-1}$, and T is the temperature (K).

3.4 Radiation and gas phase scheme

Photolysis rates are calculated off-line from reported absorption cross-sections and quantum yields using a 2-stream radiative transfer code (Thompson, 1984), where the irradiance reaching the surface is computed after photon attenuation through fifty 1 km layers in the atmosphere.

Some species in the model are constrained to their typical values measured during the Chemistry of the Antarctic Boundary Layer and Interface with Snow (CHABLIS) measurement field campaign that took place at Halley Bay in coastal Antarctica (Jones et al., 2007; Read et al., 2007), with diurnal mixing ratio profiles peaking at [CO] = 35 ppb; [DMS] = 80 pptv; [SO$_2$] = 15 pptv; [CH$_4$] = 1750 ppb; [CH$_3$CHO] = 150 pptv; [HCHO] = 150 pptv; [isoprene] = 60 pptv; [propane] = 25 pptv; [propene] = 15 pptv. During the model simulations all other species are allowed to vary. The model is solved using a variable step-size fourth-order Runge–Kutta integrator.

The heterogeneous recycle rate of a species on airborne sea-salt aerosols is calculated using the free molecular transfer approximation $k_t = 0.25\gamma cA$, where γ are the uptake coefficients whose values for the different species are taken from Atkinson et al. (2006), c is the root mean square molecular speed, and A is the effective available surface area, 10^{-7} cm^2 cm^{-3} (von Glasow et al., 2002) chosen to be typical of remote oceanic conditions. The dry deposition of a species i is computed as $V_i C_i(t)/H$, where C is the concentration of a gaseous species at a given time and V_i is the deposition velocity of species over a fixed boundary layer over time with a depth H of 400 m.

4   Proposed mechanism for iodine release from sea-ice

The mechanism is broadly illustrated in Fig. 1. Briefly, the process includes: release of iodine, in the equilibrium form of HOI+I$^-$+H$^+$ $\leftrightarrow$ I$_2$+H$_2$O, from sea-ice algae; thereafter, diffusion through brine channels to accumulate in the QLL of the ice surface accompanied by deposition and recycle of atmospheric iodine species on the QLL. Note, although we focus on inorganic iodine, organic iodine would also be transported through brine channels. Figure 2 shows a simplified quantitative schematic of the mechanism and model structure. The mechanism is based on three characteristics that separately have been reported to occur in the Antarctic springtime sea-ice environment:

(i) The Southern Ocean contains the largest quantity of micro-algae/diatoms (phytoplankton bloom) in the world (Thomas and Dieckmann, 2003). Antarctic sea-ice

covers an extensive portion of the Earth's surface – that is, a maximum extent of $\sim 4\% = 19 \times 10^6\,km^2$ in winter and minimum extent of $\sim 1\% = 5 \times 10^6\,km^2$ in summer and is accompanied to a significant degree by biological activity; it, therefore, represents one of the principal biomes on Earth (Thomas and Dieckmann, 2003).

It is known that micro-algae populations colonize the underside of sea-ice (at the seawater–sea-ice interface) and within the brine channels up to the top of sea-ice column (Thomas and Dieckmann, 2003). Via pre-concentration processes, these organisms contain enhanced concentrations of iodine up to 1000 micro-algae (e.g., *Porosira glacialis/Achnanthes* cf. *longipes*, Hill and Manley, 2009) and 30 000 macro-algae (e.g., *Laminaria digitata,* Küpper et al., 1998) times the iodine levels in the surrounding seawater (e.g. $[I^-]_{seawater} \sim 10^{-7}$ M). Iodide (I^-) accumulates to these high concentrations by way of a facilitated-diffusion process, by which efficient transport and iodine uptake from natural seawater into macro and microalgal cells occurs, independent of its electrochemical potential gradient (Küpper et al., 1998). Additionally, in the extracellular domain, haloperoxidases, membrane-bound enzymes or cell wall oxidases, along with probable intracellular sources, produce a constant flow of H_2O_2 in the apoplast of cells. Therefore, within the cells, haloperoxidases act as catalysts for the physiological oxidation of I^- into I^+ (i.e., HOI) (Vilter, 1995), Reaction (R1), which can then cross the plasma membrane. Apoplastic H_2O_2, is also consumed for the oxidation of I^- into I_2. The oxidative formation of HOI in the apoplast leads to a strong iodine solution in free diffusive contact with the surrounding seawater. Upon oxidative stress, this iodine reservoir is mobilized and a rapid, massive efflux of iodine occurs. Oxidation of iodide results in the evolution of molecular iodine and volatile halogenated compounds. In other words, HOI forms I_2 via further reaction with I^-, as shown in Reaction (R2), until equilibrium (2, −2) is achieved (e.g. Lobban et al., 1985; Küpper et al., 1998; Hill and Manley, 2009).

$$I^- + H_2O_2 \leftrightarrow HOI + OH^- \tag{R1}$$
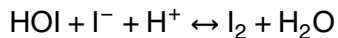
$$HOI + I^- + H^+ \leftrightarrow I_2 + H_2O \tag{R2}$$

There have been a number of laboratory studies reporting that algae releases organic and inorganic iodine after light-, chemical- and oxidative-induced stress (e.g. McFiggans et al., 2004 and references therein; Palmer et al., 2005; Hill and Manley, 2009).

During the springtime, solar radiation can penetrate through the relatively thin Southern Ocean's sea-ice layer (see below) and sea-ice fractures reaching the micro-algae colonies that populate underneath and within sea-ice. In order to account for a diurnal pattern in the light-induced iodine emissions from marine algae (Hill and Manley, 2009) the model includes a parameterization of the iodine flux from the algae colonies following the diurnal variation in actinic flux. We initialize the model using a biological pre-concentration of 10^{-4} M iodide (micro-algae, Hill and Manley, 2009).

(ii) The brine channels within sea-ice and the QLL at the sea-ice–air interface. Following solar radiation incidence upon the algae colonies and subsequent light-induced stress, intracellular iodine, equilibrated between HOI, I^- and I_2, effluxes into brine channels of sea-ice, and then diffuses up to the QLL, where it accumulates. The upward diffusion through the brine channels is driven by an iodine concentration gradient. This gradient arises from the concentration difference between the iodine emission point (e.g. algae colonies) and the iodine content in the QLL, which is that in seawater. For example, the upper limit for the concentration gradient can be up to $\sim 10^{-4}$ M between the QLL ($[I^-] \sim 10^{-7}$ M) and the iodine source in the algae colonies ($[I^-]$ up to 10^{-3} M).

Note that algae populations colonize the brine channel surfaces well into the interior of the sea-ice, close to the top of the sea-ice layer (Thomas and Dieckmann, 2003). Hence, due to the occurrence of sea-ice fractures, following springtime warming, it is also likely that during the process of sea-ice thinning and breakage the algae colonies in the upper part of the sea-ice layer will only be covered by a thin water film or be directly exposed to air.

(iii) The comparatively thin Antarctic sea-ice (mean sea-ice thickness ~ 50 cm) (Thomas and Dieckmann, 2003) allows for the relatively fast diffusion (see below) of

iodine through sea-ice brine channels and further release of $I_{2(g)}$, in addition to other iodine species, such as, $IBr_{(g)}$ and $ICl_{(g)}$, from the QLL to the atmosphere. In the model we use Fick's laws of diffusion, and diffusion coefficients for snow/ice (Shaw et al., 2011; Loose et al., 2011) to compute the strength of the iodine flux, J, as a function of iodine concentration gradient variability with time. Iodine fluxes are then obtained by incorporating D (from 10^{-4} to 10^{-7} cm^2 s^{-1}) into Fick's first law of diffusion (Shaw et al., 2011; Loose et al., 2011). Hence, for the typical Antarctic sea-ice thickness (50 cm) we calculate depth-dependent diffusion timescales (Table 1). Relevant diffusion timescales range from 52 days at 30 cm ($D = 5 \times 10^{-5}$ cm^2 s^{-1}) days to 2.4 h at 2.5 cm ($D = 1.3 \times 10^{-4}$ cm^2 s^{-1}) (Table 1). According to Eqs. (8) and (9), the iodine flux will decrease with time as the iodine concentration gradient decreases due to accumulation of iodine in the QLL.

We estimate iodine loss via measured loss rates of volatile organic iodinated compounds (VOICs – CH_3I, C_2H_5I, C_3H_7I, and C_3H_7I) assuming a VOIC concentration of $\sim 10^{-5}$ M (Shaw et al., 2011). Maximum loss rates for each of these compounds were ~ 2.1 nM h^{-1} ~ 583 femto-Molar s^{-1}). Given the range of iodine measured in algae (i.e., 10^{-7} to 10^{-3} M) and under an unlikely scenario (as iodine is replenished within micro-algae) of no iodine replenishment in micro-algae in conjunction with estimated VOIC loss rates: (1) at 10^{-7}, 10^{-5}, and 10^{-3} M initial micro-algae iodine concentration, iodine in the form of VOICs would be depleted in ~ 4, 417, and 42 000 days, respectively. This unlikely baseline scenario shows that the loss of iodine in the form of VOICs will not affect the concentration of iodine emitted from micro-algae, especially at initial iodine micro-algae concentrations above 10^{-5} M. Additional losses of I_2 and HOI via reaction with organic compounds are discussed in Sect. 6.

Therefore, even though our conservative model conditions show to be sufficient for significant iodine release, it is possible that the iodine concentration gradient between algae colonies and QLL is larger than that used in this study. For example, Hill and Manley (2009) showed that polar diatoms were especially active in releasing iodine species – specifically, releasing 0.02–2.7 µmol HOI [mg total chlorophyll]$^{-1}$ h^{-1}, at 100 µmol L^{-1}

iodide concentration. Note that $100\,\mu mol\,L^{-1}$ iodide is one-order of magnitude larger than the iodide concentration used here in the CON-AIR model. One factor that can influence the concentration gradient is the vertical extent of the algae populations within the brine channels. For instance, the closer the algae colonies are to the sea-ice surface the lesser the possible losses of iodine from reaction with organics in seawater during diffusion through brine channels and the shorter the diffusion timescale for iodine to reach the QLL (Table 1).

5 Model simulations and discussion

The model is initialized in October at local midnight at 75° S in the Southern Hemisphere springtime. Figure 3 shows simulations of iodine exchange between the QLL and the atmosphere as a function of time. This figure considers a diffusion timescale of 6 days ($D = 5 \times 10^{-5}\,cm^2\,s^{-1}$ at $\sim 10\,cm$ and $D = 1.3 \times 10^{-4}\,cm^2\,s^{-1}$ at $\sim 12.5\,cm$) to release enough iodine precursors to reach the IO levels (i.e. up to 20 pptv) observed in coastal Antarctica (Saiz-Lopez et al., 2007a; Schönhardt et al., 2008, 2012; Atkinson et al., 2012). Note however that the IO concentration peak measured during a year-round campaign at Halley Bay station occurred on 21 October (Saiz-Lopez et al., 2007), that is about 70 days after spring sunrise at coastal Antarctica. The simulations in Fig. 3a show that the nocturnal gas-phase I_2 can reach concentrations of 7×10^8 molecule cm^{-3} over the course of six days, whereas daytime I_2 concentrations are much smaller due to its fast rate of photolysis to form I atoms (Saiz-Lopez et al., 2004). Figure 3b shows that the predicted I^- concentration in the QLL increases by 2 orders of magnitude after six days of simulation due to the upward flux of iodine from the algal colonies and the accumulation in the QLL. $I_{2(aq)}$ increases at a similar rate to I^- since it forms primarily from Reaction (R2). Following Eq. (7), for a $[I_{2(aq)}] \sim 2 \times 10^{-8}\,M$ we estimate a transfer rate of I_2 from the QLL to the gas phase

of $\sim 1.5 \times 10^5$ molecules cm^{-3} s^{-1}. The concentration of IBr$_{(aq)}$, which forms from the reaction of Br$^-$ with HOI, also increases in the QLL in step with the increase of HOI.

Model simulations were run with a QLL pH value of 8, similar to ocean water. We have also assumed acidification of the QLL and model runs for pH 4 have shown a small enhancement in the release of gas phase I$_2$. As the model simulation evolves with time, the strength of the iodine flux from the phytoplankton and the iodine concentration increase in the QLL will be the mayor drivers determining the timescale as well as the concentrations of photolabile reactive iodine precursors released from sea-ice.

Also note that as the Antarctic springtime progresses, there are two factors enhancing the accumulation of I$^-$ in the QLL: (i) the phytoplankton bloom associated with high iodine emissions and increase in solar irradiance reaching the sea-ice surface, (ii) the thinning of the sea-ice and more frequent occurrence of brine channels favoring faster upward transport through the ice; and the break-up of sea-ice, which exposes phytoplankton colonies, and their associated iodine emission, directly to the atmosphere.

Figure 4 shows an example of the gas phase chemistry resulting from I$_2$ release to the atmosphere, following the model run conditions shown in Fig. 3. Atomic iodine reacts with atmospheric O$_3$ to form IO, and this radical then self-reacts to yield OIO. The calculated concentrations of IO can reach 2×10^8 molecules cm^{-3}; these levels are in good agreement with average boundary layer concentrations of the molecule recently measured at coastal Antarctica both from the ground (Saiz-Lopez et al., 2007a; Atkinson et al., 2012) and from satellite platforms (Schönhardt et al., 2008, 2012). The computed O$_3$, also plotted in Fig. 4a, shows a substantial rate of depletion due to iodine chemistry of 0.25 ppb h^{-1}. This is almost twice as fast as that calculated from bromine-mediated chemistry alone (0.14 ppb h^{-1} for typical Antarctic springtime boundary layer BrO mixing ratios of 10 pptv). Figure 4b shows the diurnal profiles of gas-phase HOI, HI and IONO$_2$. These three species can be deposited back from the gas phase onto the sea-ice surface and subsequently converted to aqueous HOI. The set of reactions involved is summarized as follows (iodine species are in the gas phase unless indi-

cated):

$$HOI \rightarrow HOI_{(aq)} \tag{R.3}$$
$$HOI_{(aq)} + I^- + H^+ \rightarrow I_{2(aq)} + H_2O \tag{R.4}$$
$$I_{2(aq)} \rightarrow I_2 \tag{R.5}$$
$$I_2 + h\nu \rightarrow 2I \tag{R.6}$$
$$2(I + O_3) \rightarrow 2(IO + O_2) \tag{R.7}$$
$$2(IO + HO_2) \rightarrow 2HOI + 2O_2 \tag{R.8}$$
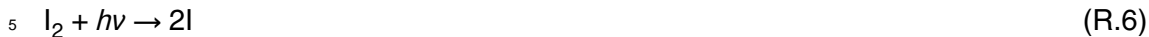
Another point to consider is that this mechanism potentially establishes a synergy between the biologically-induced emissions of iodine and the trigger of bromine release from Antarctic sea-ice. The model results show that the increase in iodine content in the QLL will also trigger the catalytic release of bromine from sea-ice via formation and subsequent release of IBr to the gas phase (see Fig. 3), which following photolysis will provide a source of reactive bromine in the Antarctic atmosphere.

We also propose that similar to the inorganic iodine release mechanism, algal emissions of iodocarbons followed by transport and accumulation in the top of the sea-ice layer may arise in phase equilibration of organic iodine from ice-covered ocean areas to the atmosphere.

Finally, we suggest that this mechanism is more efficient for the Antarctic sea-ice environment than for the Arctic due to physical constraints such as greater mean sea-ice thickness (e.g., ∼ 3 m) and smaller algal population in the Arctic (Thomas and Dieckmann, 2003). Due to the non-linearity in the system (see Eqs. 8 and 9), our calculations show that the diffusion timescale of iodine species through Arctic sea-ice is ∼ 40 times slower than that in the Antarctic. This is an upper limit for Arctic iodine emissions through the proposed mechanism since algal colonies are less predominant in the Arctic than in the Antarctic and propagation of solar irradiance through ice will also be largely limited due to thicker sea-ice. This will greatly limit the overall metabolic production of iodine species. However, it cannot be ruled out that when the Arctic sea-ice

melts the phytoplankton colonies will be directly exposed to air and therefore constitute a potential source of iodine in the Arctic atmosphere. The difference in Arctic and Antarctic sea-ice microstructure – that is, predominantly columnar ice in the Arctic vs. frazil and platelet ice in Antarctica.

6   Uncertainties and future work

Although it is beyond the scope of this manuscript, below we discuss additional loss and production pathways for iodine and VOICs within sea-ice (Table 2), which should be addressed in future model studies.

1. Reactions of I_2 and HOI with dissolved organic matter (DOM) in sea-ice/snow. Assuming I_2 concentrations of $\sim 10^{-7}$, 10^{-5} and 10^{-3} M and a first-order loss rate $\sim 7 \times 10^{-3} \, s^{-1}$ (for coastal water) and $5 \times 10^{-5} \, s^{-1}$ (for open water) of I_2 with dissolved organic matter (DOM) (Truesdale, 1995; Carpenter et al., 2013), the lifetime (without replenishment) of I_2 would be ~ 2.4 and ~ 333 min, respectively. We will also investigate the equilibrium reaction of $I_2 + I^- \leftrightarrow I_3^-$ (O'Driscoll, 2008), whose equilibrium lies well to the right, forming the trihalide ion; still, its forward reaction rate is 3 orders of magnitude slower than the primary reaction releasing I_2 – that is, $HOI + I^- + H^+ \leftrightarrow I_2 + H_2O$.

2. Abiotic release of iodine from water surfaces; for instance, Chance et al. (2010) observed surface seawater iodide levels of up to 150 nM in summer off the coastal western Antarctic peninsula. Heterogeneous reaction with 30 ppb atmospheric ozone could release $\sim 2 \times 10^7$ molecules cm^{-2} s^{-1} for I_2 and 3.5×10^8 molecules cm^{-2} s^{-1} for HOI from $O_3 + I^-$ (Carpenter et al., 2013).

3. Via haloperoxidase activity, biogenic emissions of iodine are another viable release mechanism. Under optimum assay conditions using *Porosira glacialis*, a centric diatom, Hill and Manley (2009) observed release rates up to

271 fmol HOI cell^{-1} h^{-1}. Estimated production rates are highly dependent on the amount of biomass, as well as I$^-$ and H$_2$O$_2$ concentrations. Much lower activity was observed at iodide concentrations closer to natural seawater. Based on data shown in Hill and Manley (2009), release rates may be a factor of 100 lower under ambient H$_2$O$_2$ and iodide conditions, e.g. ~ 0.03 µmol HOI [mg total Chl]$^{-1}$ h^{-1}. Using representative chlorophyll concentrations from Sturges et al. (1997) yields a very high production rate of $\sim 1 \times 10^{10}$ molecules cm^{-2} s^{-1} HOI. The majority of the biomass producing this will be at the base of the ice, therefore losses of HOI will occur before release to the atmosphere.

4. Production of organic iodine within leads and polynyas and near sea-ice. To explain the atmospheric levels of organoiodines and IO at Hudson Bay, Mahajan et al. (2010) postulated CH$_2$I$_2$ = 1×10^6 molecule cm^{-2} s^{-1}, CH$_2$IBr = 2×10^9 molecule cm^{-2} s^{-1}, CH$_2$ICl = 5×10^7 molecule cm^{-2} s^{-1}, and CH$_3$I = 2×10^8 molecule cm^{-2} s^{-1} from open leads 15 h upwind of measurements. At Hudson Bay, Carpenter et al. (2005) measured high concentrations (i.e., ~ 1–3 pptv) of reactive dihalomethanes. Yet, organic iodine compounds are not ubiquitously high in polar regions (Carpenter et al., 2007; Atkinson et al., 2012; Granfors et al., 2015).

7 Summary and conclusions

A mechanism for iodine release from sea-ice has been proposed. This mechanism incorporates the coupling between stress-induced biological emissions of iodine, diffusion of iodine through sea-ice and phase equilibration to the atmosphere. In order to quantitatively investigate the feasibility of the mechanism a multiphase chemical model has been developed. Model simulations for the coastal Antarctic springtime show that the release of photolabile inorganic iodine (i.e. I$_2$, IBr, ICl) could account for the observations of elevated IO in this environment, which is primarily sourced near the surface of

sea-ice (i.e., $\geq 30\,\text{cm}$ for $D = 5.5 \times 10^{-5}\,\text{cm}^2\,\text{s}^{-1}$ and $\geq 50\,\text{cm}$ at $D = 1.3 \times 10^{-4}\,\text{cm}^2\,\text{s}^{-1}$). Most likely, the overall mechanism involves a combination of biological emissions of iodine simultaneously at different depths within the sea-ice column. This process may also trigger reactive bromine release from sea-ice via gas phase equilibration and sub-

5 sequent photolysis of IBr. In addition, following the same mechanism, organic iodine may also be released from sea-ice to the atmosphere. Lastly, it appears that coastal Antarctic sea-ice is not alone in emitting iodine as recent measurements have reported $3.4 \pm 1.2\,\text{pptv}$ IO in the Arctic over open water polynas that form in the sea-ice (Mahajan et al., 2010). The smaller amounts of IO measured over the Arctic may be indicative of

10 differences in Arctic vs. Antarctic sea-ice thickness, micro-algae amount, sea-ice microstructure, salinity, porosity, and temperature. Therefore, this mechanism may also govern the emission of iodine (including VOICs) measured in the Artic as well. We also acknowledge here that the efflux of HOI and I^- via diatoms/micro-algae likely forms I_2 rapidly as a function of depth, which could also be coupled to the diffusion of I^- and

15 HOI to the top layers to be released at the surface; this possibility (given the rapid forward reaction of $HOI_{(aq)} + I^- + H^+ \rightarrow I_{2(aq)} + H_2O$) may also give insight into lower I^- concentrations measured in brine channels compared to its pre-concentration in algae.

The Supplement related to this article is available online at doi:10.5194/acpd-15-10257-2015-supplement.

We are grateful to J. Plane, S. Sander, R. Salawitch and R. Chance for very helpful discussions and comments on this work.

References

Arrigo, K. R. and Sullivan, C. W.: The influence of salinity and temperature covariation on the photophysiological characteristics of Antarctic sea ice microalgae, J. Phycol., 28, 746–756, 1992.

Arrigo, K. R. and Thomas, D. N.: Large scale importance of sea ice biology in the Southern Ocean, Antarct. Sci., 16, 471–486, 2004.

Atkinson, H. M., Huang, R.-J., Chance, R., Roscoe, H. K., Hughes, C., Davison, B., Schön-hardt, A., Mahajan, A. S., Saiz-Lopez, A., Hoffmann, T., and Liss, P. S.: Iodine emissions from the sea ice of the Weddell Sea, Atmos. Chem. Phys., 12, 4–6, doi:10.5194/acpd-12-11595-2012, 2012.

Atkinson, R., Baulch, D. L., Cox, R. A., Crowley, J. N., Hampson, R. F., Hynes, R. G., Jenkin, M. E., Rossi, M. J., Troe, J., and IUPAC Subcommittee: Evaluated kinetic and photochemical data for atmospheric chemistry: Volume II – gas phase reactions of organic species, Atmos. Chem. Phys., 6, 3625–4055, doi:10.5194/acp-6-3625-2006, 2006.

Barrie, L. A., Bottenheim, J. W., Schnell, R. C., Crutzen, P. J., and Rasmussen, R. A.: Ozone destruction and photochemical reactions at polar sunrise in the lower Arctic atmosphere, Nature, 334, 138–141, 1988.

Bloss, W. J., Lee, J. D., Johnson, G. P., Sommariva, R., Heard, D. E., Saiz-Lopez, A., Mc-Figgans, G., Coe, H., Flynn, M., Williams, P., Rickard, A. R., and Fleming, Z. L.: Impact of halogen monoxide chemistry upon boundary layer OH and HO_2 concentrations at a coastal site, Geophys. Res. Lett., 32, L06814, doi:10.1029/2004GL022084, 2005.

Boxe, C. S.: Nitrate Photolysis and Interrelated Chemical Phenomenon in Ice, Thesis, California Institute of Technology, Pasadena, California, 2005.

Boxe, C. S. and Saiz-Lopez, A.: Multiphase modeling of nitrate photochemistry in the quasi-liquid layer (QLL): implications for NO_x release from the Arctic and coastal Antarctic snowpack, Atmos. Chem. Phys., 8, 4855–4864, doi:10.5194/acp-8-4855-2008, 2008.

Boxe, C. S., Colussi, A. J., Hoffmann, M. R., Tan, D., Mastromarino, J., Case, A. T., Sandholm, S. T., and Davis, D. D.: Multiscale ice fluidity in NO_x photodesorption from frozen nitrate solutions, J. Phys. Chem. A, 107, 11409–11413, 2003.

Boxe, C. S., Colussi, A. J., Hoffmann, M. R., Murphy, J., Wooldridge, P., Betram, T., and Cohen, R.: Photochemical production and release of gaseous NO_2 from nitrate-doped water ice, J. Phys. Chem. A, 109, 8520–8525, 2005.

Boxe, C. S., Colussi, A. J., Hoffmann, M. R., Perez, I., Murphy, J. G., and Cohen, R. C.: Kinetics of gaseous NO and NO_2 evolution from illuminated frozen nitrate solution, J. Phys. Chem. A, 110, 3578–3583, 2006.

Brierley, A. S. and Thomas, D. N.: Ecology of Southern Ocean pack ice, Adv. Mar. Biol., 43, 171–276, 2002.

Burkholder, J. B., Curtius, J., Ravishankara, A. R., and Lovejoy, E. R.: Laboratory studies of the homogeneous nucleation of iodine oxides, Atmos. Chem. Phys., 4, 19–34, doi:10.5194/acp-4-19-2004, 2004.

Calvert, J. G. and Lindberg, S. E.: The potential influence of iodine-containing compounds on the chemistry of the troposphere in the polar spring, I. Ozone depletion, Atmos. Environ., 38, 5087–5104, 2004a.

Calvert, J. G. and Lindberg, S. E.: The potential influence of iodine-containing compounds on the chemistry of the troposphere in the polar spring, II. Mercury depletion, Atmos. Environ., 38, 5105–5116, 2004b.

Carpenter, L. J., Wevill, D. J., Palmer, C. J., and Michels, J.: Depth profiles of volatile iodine and bromine-containing halocarbons in coastal Antarctic waters, Mar. Chem., 103, 227–236, 2007.

Carpenter, L. J., MacDonald, S. M., Shaw, M. D., Kumar, R., Saunders, R. W., Parthipan, R., Wilson, J., and Plane, J. M. C.: Atmospheric iodine levels influenced by sea surface emissions of inorganic iodine, Nat. Geosci., 6, 108–111, doi:10.1038/NGEO1687, 2013.

Chameides, W. L. and Davis, D. D.: Iodine: its possible role in tropospheric photochemistry, J. Geophys. Res., 85, 7383–7393, 1980.

Chance, R., Weston, K., Baker, A. R., Hughes, C., Malin, G., Carpenter, L., Meredith, M. P., Clarke, A., Jickells, T. D., Mann, P., and Rossetti, H.: Seasonal and interannual variation of dissolved iodine speciation at a coastal Antarctic site, Mar. Chem., 118, 171–181, 2010.

Delille, B.: Inorganic carbon dynamics and air-ice-sea CO_2 fluxes in the open and coastal waters of the Southern Ocean, PhD thesis, University of Liege, 2006.

A mechanism for biologically-induced iodine emissions from sea-ice

A. Saiz-Lopez et al.

Title Page

Abstract	Introduction
Conclusions	References
Tables	Figures

◄ | ►

◄ | ►

Back | Close

Full Screen / Esc

Printer-friendly Version

Interactive Discussion

Deming, J. W.: Psychrophiles and polar regions, Curr. Opin. Microbiol., 5, 301–309, doi:10.1016/S1369-5274(02)00329-6, 2002.

Dubowski, Y., Colussi, A. J., Boxe, C. S., and Hoffmann, M. R.: Monotonic increase of nitrite yields in the photolysis of nitrate in ice and water between 238 and 294 K, J. Phys. Chem. A, 106, 6967–6971, 2002.

Eicken, H.: The role of sea ice in structuring Antarctic ecosystems, Polar Biol., 12, 3–13, 1992a.

Eicken, H.: Salinity profiles of Antarctic sea ice: field data and model results, J. Geophys. Res., 97, 15545–15557, 1992b.

Eicken, H.: From the microscopic to the macroscopic to the regional scale: growth, microstructure and properties of sea ice, in: Sea Ice – An Introduction to its Physics, Biology, Chemistry and Geology, edited by: Thomas, D. N. and Dieckmann, G. S., Blackwells Scientific Ltd., London, 22–81, 2003a.

Eicken, H.: The Role of Arctic Sea-Ice in Transporting and Cycling Terrestrial Organic Matter, Springer-Verlag, Berlin, 45–53, 2003b.

Eicken, H.: Salinity profiles of Antarctic sea ice: field data and model results, J. Geophys. Res.-Oceans, 97, 15545–15557 doi:10.1029/92JC01588, 2012.

Friess, U., Wagner, T., Pundt, I., Pfeilsticker, K., and Platt, U.: Spectroscopic measurements of tropospheric iodine oxide at Neumayer Station, Antarctica, Geophys. Res. Lett., 24, 1941–1944, 2001.

Frankenstein, G. and Garner, R.: Equations for determining the brine volume of sea ice from −0.5 to −22.9 °C, J. Glaciol., 6, 943–944, 1967.

Gálvez, O., Gómez Martín, J. C., Gómez, P. C., Saiz-Lopez, A., and Pacios, L. F.: A theoretical study on the formation of iodine oxide aggregates and monohydrates., Phys. Chem. Chem. Phys., 15, 15572–15583, doi:10.1039/c3cp51219c, 2013.

Gleitz, M. and Thomas, D. N.: Physiological responses of a small Antarctic diatom (*Chaetoceros* sp.) to simulated environmental constraints associated with sea ice formation, Mar. Ecol.-Prog. Ser., 88, 271–278, 1993.

Gleitz, M., Rutgers, v. d. L. M., Thomas, D. N., Dieckmann, G. S., and Millero, F. M.: Comparison of summer and winter inorganic carbon, oxygen and nutrient concentrations in Antarctic sea ice brine, Mar. Chem., 51, 81–91, 1995.

Golden, K. M., Ackley, S. F., and Lytle, V. I.: The percolation phase transition in sea ice, Science, 282, 2238–2241, 1998.

Title Page

Abstract | Introduction

Conclusions | References

Tables | Figures

|◄ | ►|

◄ | ►

Back | Close

Full Screen / Esc

Printer-friendly Version

Interactive Discussion

Golden, K. M., Eicken, H., Heaton, A., Miner, J., Pringle, D. J., and Zhu, J.: Thermal evolution of permeability and microstructure in sea ice, Geophys. Res. Lett., 34, L16501, doi:10.1029/2007GL030447, 2007.

Gómez Martín, J. C., Gálvez, O., Baeza-Romero, M. T., Ingham, T., Plane, J. M. C., and Blitz, M. A.: On the mechanism of iodine oxide particle formation, Phys. Chem. Chem. Phys., 15, 15612–15622, doi:10.1039/c3cp51217g, 2013.

Gong, S. L., Walmsley, J. L., Barrie, L. A., and Hopper, J. F.: Mechanisms for surface ozone depletion and recovery during Polar Sunrise, Atmos. Environ., 31, 969–981, 1997.

Gosink, T. A., Perason, J. G., and Kelly, J. J.: Gas movement through sea-ice, Nature, 263, 41–42, 1976.

Granfors, A., Ahnoff, M., Mills, M. M., and Abrahamsoon, K.: Organic iodine in Antarctic sea ice: a comparison between winter in the Weddell Sea and summer in the Amundsen Sea, J. Geophys. Res. Biogeosci., 119, 2276–2291, doi:10.1002/2014JG002727, 2015.

Grannas, A. M., Jones, A. E., Dibb, J., Ammann, M., Anastasio, C., Beine, H. J., Bergin, M., Bottenheim, J., Boxe, C. S., Carver, G., Chen, G., Crawford, J. H., Dominé, F., Frey, M. M., Guzmán, M. I., Heard, D. E., Helmig, D., Hoffmann, M. R., Honrath, R. E., Huey, L. G., Hutterli, M., Jacobi, H. W., Klán, P., Lefer, B., McConnell, J., Plane, J., Sander, R., Savarino, J., Shepson, P. B., Simpson, W. R., Sodeau, J. R., von Glasow, R., Weller, R., Wolff, E. W., and Zhu, T.: An overview of snow photochemistry: evidence, mechanisms and impacts, Atmos. Chem. Phys. Discuss., 7, 4165–4283, doi:10.5194/acpd-7-4165-2007, 2007.

Gravestock, T., Blitz, M. A., and Heard, D. E.: Kinetics study of the reaction of iodine monoxide radicals with dimethyl sulfide, Phys. Chem. Chem. Phys, 7, 2173–2181, 2005.

Heinesch, B., Yernaux, M., Aubinet, M., Geilfus, N.-X., Papakyriakou, T., Carnat, G., Eicken, H., Tison, H.-L., and Delille, B.: Measuring air–ice CO_2 fluxes in the Arctic, FluxLetter, 2, 9–10, 2009.

Heygster, G., Hendricks, S., Kaleschke, L., Maass, N., Mills, P., Stammer, D., Tonboe, R. T., and Haas, C.: L-Band Radiometry for Sea-Ice Applications (Technical Report), Institute of Environmental Physics, University of Bremen, ESA/ESTEC Contract N. 21130/08/NL/EL.

Hill, V. L. and Manley, S. L.: Release of reactive bromine and iodine from diatoms and its possible role in halogen transfer in polar and tropical oceans, Limnol. Oceanogr., 54, 812–822, 2009.

Hoffmann, T., O'Dowd, C. D., and Seinfeld, J. H.: Iodine oxide homogeneous nucleation: an explanation for coastal new particle production, Geophys. Res. Lett., 28, 1949–1952, 2001.

A mechanism for biologically-induced iodine emissions from sea-ice

A. Saiz-Lopez et al.

Title Page

Abstract	Introduction
Conclusions	References
Tables	Figures

◄	►
◄	►
Back	Close

Full Screen / Esc

Printer-friendly Version

Interactive Discussion

Horner, R. A. (Ed.): Ecology of sea ice microalgae, in: Sea Ice Biota, CRC Press, Boca Raton, 83–103, 1986.

Houghton, J. T., Ding, Y., Griggs, D. J., Noguer, M., van der Linden, P. J., Dai, X., Maskell, K., and Johnson, C. A. (Eds.): Climate Change 2001: The Scientific Basis, Cambridge Univ. Press, 2001.

Jimenez, J. L., Bahreini, R., Cocker, D. R., Zhuang, H., Varutbangkul, V., Flagan, R. C., Seinfeld, J. H., O'Dowd, C. D., and Hoffmann, T.: New particle formation from photooxidation of diiodomethane (CH_2I_2), J. Geophys. Res., 108, 4318, doi:10.1029/2002JD002452, 2003.

Jones, C. and Carpenter, L. J.: Solar photolysis of CH_2I_2, CH_2ICl, and CH_2IBr, Environ. Sci. Technol., 39, 6130–6137, 2005.

Jones, C. and Carpenter, L. J.: Solar photolysis of CH_2I_2, CH_2ICl, and CH_2IBr in water, saltwater, and seawater, Environ. Sci. Technol., 40, 1372–1372, 2006.

Jones, A. E., Wolff, E. W., Salmon, R. A., Bauguitte, S. J.-B., Roscoe, H. K., Anderson, P. S., Ames, D., Clemitshaw, K. C., Fleming, Z. L., Bloss, W. J., Heard, D. E., Lee, J. D., Read, K. A., Hamer, P., Shallcross, D. E., Jackson, A. V., Walker, S. L., Lewis, A. C., Mills, G. P., Plane, J. M. C., Saiz-Lopez, A., Sturges, W. T., and Worton, D. R.: Chemistry of the Antarctic Boundary Layer and the Interface with Snow: an overview of the CHABLIS campaign, Atmos. Chem. Phys., 8, 3789–3803, doi:10.5194/acp-8-3789-2008, 2008.

Kirst, G. O. and Wiencke, C.: Ecophysiology of polar algae, J. Phycol., 31, 181–189, 1995.

Krembs, C., Gradinger, R., and Spindler, M.: Implications of brine channel geometry and surface area for the interaction of sympagic organisms in Arctic sea ice, J. Exp. Mar. Ecol., 243, 55–80, 2000.

Küpper, F. C., Schweigert, N., Gall, A., Legendre, J.-M., Vilter, H., and Kloareg, B.: Iodine uptake in Laminariales involves extracellular, haloperoxidase-mediated oxidation of iodide, Planta, 207, 163–171, 1998.

Kusy, R. P. and Turner, D. T.: Electrical resistivity of a polymeric insulator containing segregated metallic particles, Nature, 229, 58–59, 1971.

Launiainen, J. and Vihma, T.: On the surface heat fluxes in the Weddell Sea, in: The Polar Oceans and Their Role in Shaping the Global Environment, Nansen Centennial Volume, edited by: Johannessen, O. M., Muench, R., and Overland, J. E., Geophys. Monog. Ser., 85, American Geophysical Union, 399–419, 1994.

Lizotte, M. P.: The microbiology of sea ice, in: Sea Ice: an Introduction to its Physics, Chemistry, Biology and Geology, edited by: Thomas, D. N. and Dieckmann, G. S., Blackwell, Oxford, 184–210, 2003.

Lobban, C. S., Harrison, P. J., and Duncan, M. J.: The Physiological Ecology of Seaweeds, Cambridge Univ. Press, Cambridge, 1985.

Loose, B., Schlosser, P., Perovich, D., Ringelberg, D., Ho, D. T., Takahashi, R., Richter-Menge, J. Richter, Reynolds, C. M., and McGillis, W. R.: Gas diffusion through columnar laboratory sea ice: implications for mixed-layer ventilation of CO_2 in seasonal ice zone, Tellus B, 63, 23–39, 2011.

Mahajan, A. S., Shaw, M., Oetjen, H., Hornsby, K. E., Carpenter, L. J., Kaleschke, L., Tian-Kunze, X., Lee, J. D., Moller, S. J., Edwards, P., Commane, R., Ingham, T., Heard, D. E., and Plane, J. M. C.: Evidence of reactive iodine chemistry in the Arctic boundary layer, J. Geophys. Res.-Atmos., 115, D20303, doi:10.1029/2009JD013665, 2010.

Maksym, T. and Jeffries, M. O.: A one dimensional percolation model of flooding and snow ice formation on Antarctic sea ice, 105, 26313–26331, 2012.

Margesin, R., Schinner, F., Marx, J.-C., and Gerday, C.: Psychrophiles: From Biodiversity to Biotechnology, Springer-Verlag Science and Business Media, Berlin, 2008.

McFiggans, G., Coe, H., Burgess, R., Allan, J., Cubison, M., Alfarra, M. R., Saunders, R., Saiz-Lopez, A., Plane, J. M. C., Wevill, D., Carpenter, L., Rickard, A. R., and Monks, P. S.: Direct evidence for coastal iodine particles from Laminaria macroalgae – linkage to emissions of molecular iodine, Atmos. Chem. Phys., 4, 701–713, doi:10.5194/acp-4-701-2004, 2004.

McFiggans, G. J. Plane, J. M. C., Allan, B. J., Carpenter, L. J., Coe, H., and O'Dowd, C. D.: A modeling study of iodine chemistry in the marine boundary layer, J. Geophys. Res.-Atmos., 105, 14371–14385, 2000.

Michalowski, B. A., Francisco, J. S., Li, S., Barrie, L. A., Bottenheim, J. W., and Shepson, P. B.: A computer model study of multiphase chemistry in the Arctic boundary layer during polar sunrise, J. Geophys. Res., 105, 15131–15145, doi:10.1029/2000JD900004, 2000.

Miller, L. A., Papakyriakou, T. N., Collins, R. E., Deming, J. W., Ehn, J. K., Macdonald, R. W., Mucci, A., Owens, O., Raudsepp, M., and Sutherland, N.: Carbon dioxide dynamics in sea-ice: winter flux time series, J. Geophys. Res., 116, C02028, doi:10.1029/2009JC006058, 2011.

Title Page

Abstract | Introduction

Conclusions | References

Tables | Figures

|◄ | ►|

◄ | ►

Back | Close

Full Screen / Esc

Printer-friendly Version

Interactive Discussion

Mock, T. and Junge, K.: Psychrophilic diatoms: mechanisms for survival in freeze–thaw cycles, in: Algae and Cyanobacteria in Extreme Environments, edited by: Seckbach, J., Springer, New York, USA, 345–364, 2007.

Mock, T. and Thomas, D. N.: Recent advances in sea-ice microbiology, Environ. Microbiol., 7, 605–619, doi:10.1111/j.1462-2920.2005.00781.x, 2005.

Mock, T. and Valentin, K. U.: Photosynthesis and cold acclimation – molecular evidence from polar diatom, J. Phycol., 40, 732–741, 2004.

Mock, T., Krell, A., Glockner, G., Kolukisaoglu, U., and Valentin, K.: Analysis of expressed sequence tags (ests) from polar diatom fragilariopsis cylindrus, J. Phycol., 42, 78–85, doi:10.1111/j.1529-8817.2006.00164.x, 2006.

Nomura, D., Eicken, H., Gradinger, R., and Shirasawa, K.: Rapid physically driven inversion of air–sea ice CO_2 flux in the seasonal landfast ice of Barrow, Alaska after onset of surface melt, Cont. Shelf Res., 30, 1998–2004, 2010a.

Nomura, D., Yoshikawa-Inoue, H., Toyota, T., and Shirasaw, K.: Effects of snow, snow melting and refreezing processes on air–sea–ice CO_2 flux, J. Glaciol., 56, 262–270, 2010b.

O'Dowd, C. D., Geever, M., and Hill, M. K.: New particle formation: nucleation rates and spatial scales in the clean marine coastal environment, Geophys. Res. Lett., 25, 1661–1664, 1998.

O'Dowd, C. D., Jimenez, J. L., Bahreini, R., Flagan, R. C., Seinfeld, J. H., Hämeri, K., Pirjola, L., Kulmala, M., Jennings, S. G., and Hoffmann, T.: Marine aerosol formation from biogenic iodine emissions, Nature, 417, 632–636, 2002.

O'Driscoll, P., Minogue, N., Takenaka, N., and Sodeau, J.: Release of nitric oxide and iodine to the atmosphere from the freezing of sea-salt aerosol components, J. Phys. Chem. A, 112, 1677–1682, 2008.

Ono, N. and Kasai, T.: Surface layer salinity of young sea ice, Ann. Glaciol., 6, 288–289, 1985.

Palmer, C. J., Anders, T. L., Carpenter, L. J., Küpper, F. C., and McFiggans, G. B.: Iodine and halocarbon response of *Laminaria digitata* to oxidative stress and links to atmospheric new particle production, Environ. Chem., 2, 282–290, 2005.

Palmer, D. A., Ramette, R. W., and Mesmer, R. E.: Triiodide ion formation equilibrium and activity coefficients in aqueous solution, 13, 673–683, 1984.

Palmisano, A. C. and Garrison, D. L.: Microorganisms in Antarctic sea-ice, in: Antarctic Microbiology, edited by: Friedman, I., Wiley-Liss, New York, 167–218. 1993.

Papakyriakou, T. and Miller, L.: Springtime CO_2 exchange over seasonal sea ice in the Canadian Arctic Archipelago, Ann. Glacio., 52, 215–224, 2011.

A mechanism for biologically-induced iodine emissions from sea-ice

A. Saiz-Lopez et al.

Title Page

Abstract | Introduction

Conclusions | References

Tables | Figures

Back | Close

Full Screen / Esc

Printer-friendly Version

Interactive Discussion

Pechtl, S., Lovejoy, E. R., Burkholder, J. B., and von Glasow, R.: Modeling the possible role of iodine oxides in atmospheric new particle formation, Atmos. Chem. Phys., 6, 505–523, doi:10.5194/acp-6-505-2006, 2006.

Petrenko, V. F. and Whitworth, R. W.: Physics of Ice, University Press, Oxford, 1999.

Read, K. A., Lewis, A. C., Salmon, R. A., Jones, A. E., and Bauguitte, S.: OH and halogen atom influence on the variability of non-methane hydrocarbons in the Antarctic Boundary Layer, Tellus B, 59, 22–38, 2007.

Read, K. A., Mahajan, A. S., Carpenter, L. J., Evans, M. J., Faria, B. V. E., Heard, D. E., Hopkins, J. R., Lee, J. D., Moller, S. J., Lewis, A. C., Mendes, L., McQuaid, J. B., Oetjen, H., Saiz-Lopez, A., Pilling, M. J., and Plane, J. M. C.: Extensive halogen-mediated ozone destruction over the tropical Atlantic Ocean, Nature, 453, 1232–1235, 2008.

Saito, T. and Ono, N.: Percolation in sea ice, I. Measurements of kerosene permeability of NaCl ice, LTS-A, 37, 55–62, 1978.

Saiz-Lopez, A. and Plane, J. M. C.: Novel iodine chemistry in the marine boundary layer, Geophys. Res. Lett., 31, L04112, doi:10.1029/2003GL019215, 2004.

Saiz-Lopez, A. and von Glasow, R.: Reactive halogen chemistry in the troposphere., Chem. Soc. Rev., 41, 6448–6472, doi:10.1039/c2cs35208g, 2012.

Saiz-Lopez, A., Saunders, R. W., Joseph, D. M., Ashworth, S. H., and Plane, J. M. C.: Absolute absorption cross-section and photolysis rate of I_2, Atmos. Chem. Phys., 4, 1443–1450, doi:10.5194/acp-4-1443-2004, 2004.

Saiz-Lopez, A., Plane, J. M. C., McFiggans, G., Williams, P. I., Ball, S. M., Bitter, M., Jones, R. L., Hongwei, C., and Hoffmann, T.: Modelling molecular iodine emissions in a coastal marine environment: the link to new particle formation, Atmos. Chem. Phys., 6, 883–895, doi:10.5194/acp-6-883-2006, 2006.

Saiz-Lopez, A., Mahajan, A. S., Salmon, R. A., Bauguitte, S. J. B., Jones, A. E., Roscoe, H. K., and Plane, J. M. C.: Boundary layer halogens in coastal Antarctica, Science, 20, 348–351, 2007a.

Saiz-Lopez, A., Chance, K., Liu, X., Kurosu, T. P., and Sander, S. P.: First observations of iodine oxide from space, Geophys. Res. Lett., 34, L12812, doi:10.1029/2007GL030111, 2007b.

Saiz-Lopez, A., Plane, J. M. C., Mahajan, A. S., Anderson, P. S., Bauguitte, S. J.-B., Jones, A. E., Roscoe, H. K., Salmon, R. A., Bloss, W. J., Lee, J. D., and Heard, D. E.: On the vertical distribution of boundary layer halogens over coastal Antarctica: implications for O_3, HO_x, NO_x and the Hg lifetime, Atmos. Chem. Phys., 8, 887–900, doi:10.5194/acp-8-887-2008, 2008.

Title Page

Abstract | Introduction

Conclusions | References

Tables | Figures

◄ | ►

◄ | ►

Back | Close

Full Screen / Esc

Printer-friendly Version

Interactive Discussion

Saiz-Lopez, A., Lamarque, J.-F., Kinnison, D. E., Tilmes, S., Ordóñez, C., Orlando, J. J., Conley, A. J., Plane, J. M. C., Mahajan, A. S., Sousa Santos, G., Atlas, E. L., Blake, D. R., Sander, S. P., Schauffler, S., Thompson, A. M., and Brasseur, G.: Estimating the climate significance of halogen-driven ozone loss in the tropical marine troposphere, Atmos. Chem. Phys., 12, 3939–3949, doi:10.5194/acp-12-3939-2012, 2012.

Saiz-Lopez, A., Fernandez, R. P., Ordóñez, C., Kinnison, D. E., Gómez Martín, J. C., Lamarque, J.-F., and Tilmes, S.: Iodine chemistry in the troposphere and its effect on ozone, Atmos. Chem. Phys., 14, 13119–13143, doi:10.5194/acp-14-13119-2014, 2014.

Saunders, R. W. and Plane, J. M. C.: Formation pathways and composition of iodine ultra-fine particles, Environ. Chem., 2, 299–303, 2005.

Saunders, R. W. and Plane, J. M. C.: Fractal growth modelling of I_2O_5 nanoparticles, J. Aerosol Sci., 37, 1737–1749, 2006.

Schnack-Schiel, S. B.: The macrobiology of sea ice, in: Sea Ice. An introduction to its Physics, Chemistry, and Geology, edited by: Thomas, D. N. and Dieckmann, G. S., Blackwell Science, 211–239, 2003.

Schönhardt, A., Richter, A., Wittrock, F., Kirk, H., Oetjen, H., Roscoe, H. K., and Burrows, J. P.: Observations of iodine monoxide columns from satellite, Atmos. Chem. Phys., 8, 637–653, doi:10.5194/acp-8-637-2008, 2008.

Schönhardt, A., Begoin, M., Richter, A., Wittrock, F., Kaleschke, L., Gómez Martín, J. C., and Burrows, J. P.: Simultaneous satellite observations of IO and BrO over Antarctica, Atmos. Chem. Phys., 12, 6565–6580, doi:10.5194/acp-12-6565-2012, 2012.

Schwerdtleger, W.: The Antarctic Peninsula and the temperature regime of the Weddell Sea, Antarct. J. US, 9, 213–214, 1974.

Sellegri, K., Loon, Y. J., Jennings, S. G., O'Dowd, C. D., Pirjola, L., Cautenet, S., Chen, H. W., and Hoffmann, T.: Quantification of coastal new ultra-fine particles formation from in situ and chamber measurements during the BIOFLUX campaign, Environ. Chem., 2, 260–270, 2005.

Semiletov, I., Makshtas, A., Akasofu, S.-I., and Andreas, E. L.: Atmospheric CO_2 balance: the role of Arctic sea ice, Geophys. Res. Lett., 31, L05121, doi:10.1029/2003GL017996, 2004.

Shaw, M. D., Carpenter, L. J., Baeza-Romero, M. T., and Jackson, A. V.: Thermal evolution of diffusive transport of atmospheric halocarbons through artificial sea-ice, Atmos. Environ., 45, 6393–6402, 2011.

Sommariva, R. and von Glasow, R.: Multiphase halogen chemistry in the tropical atlantic ocean, Environ. Sci. Technol., 46, 10429–10437, doi:10.1021/es300209f, 2012.

A mechanism for biologically-induced iodine emissions from sea-ice

A. Saiz-Lopez et al.

Title Page

Abstract | Introduction

Conclusions | References

Tables | Figures

◀ | ▶

◁ | ▷

Back | Close

Full Screen / Esc

Printer-friendly Version

Interactive Discussion

Sommer, U.: Maximum growth rates of Antarctic phytoplankton: only weak dependence on cell size, Limnol. Oceanogr., 34, 1109–1112, 1989.

Solomon, S., Garcia, R. R., and Ravishankara, A. R: On the role of iodine in ozone depletion, J. Geophys. Res., 99, 20491–20500, 1994.

5 Sturges, W. T., Cota, G. F., and Buckley, P. T.: Vertical profiles of bromoform in snow, sea ice, and seawater in the Canadian Arctic, J. Geophys. Res., 102, 25073–25083, 1997.

Thomas, D. N. and Dieckmann, G. S.: Sea Ice: An Introduction to its Physics, Chemistry, Biology, and Geology, Blackwell, Oxford, 2003.

Thompson, A. M.: The effect of clouds on photolysis rates and ozone formation in the unpolluted
10 troposphere, J. Geophys. Res., 89, 1341–1349, 1984.

Truesdale, V. W., Luther III, G. W., and Canosa-Mas, C.: Molecular iodine reduction in seawater: an improved rate equation considering organic compounds, Mar. Chem., 48, 143–150, 1995.

Tucker III, W. B., Perovich, D. K., Gow, A. J., Weeks, W. F., and Drinkwater, M. R.: Physical properties of sea ice relevant to remote sensing, in: Microwave Remote Sensing of Sea
15 Ice, Chap. 2, edited by: Carsey, F. D., Geophys. Monolog. 68, American Geophysical Union, Washington, DC, 462 pp., 1993.

Ulaby, F. T., Moore, R. K., and Fung, A. K.: Microwave Remote Sensing, Active and Passive, Addison Wesley, London, England, 1986.

Vancoppenolle, M., Fichefet, T., and Goose, H.: Simulating the mass balance and salinity of
20 Arctic and Antarctic sea ice. 2. Importance of sea ice salinity variations, Ocean Model., 27, 54–69, 2009.

Veihelmann, B., Olesen, F. S., and Kottmeier, C.: Sea ice surface temperature in the Weddell Sea (Antarctica), from drifting buoy and AVHRR data, Cold Reg. Sci. Technol., 33, 19–27, 2001.

25 Vilter, H.: Metal Ions in Biological Systems, Vanadium and its Role in Life: Vanadium-Dependent Haloperoxidases, Dekker, New York, 1995.

Vogt, R., Crutzen, P. J., and Sander, R.: A mechanism for halogen release from sea-salt aerosol in the remote marine boundary layer, Nature, 383, 327–330, 1996.

Vogt, R., Sander, R., von Glasow, R., and Crutzen, P. J.: Iodine chemistry and its role in halogen
30 activation and ozone loss in the marine boundary layer: a model study, J. Atmos. Chem., 32, 375–395, 1999.

A mechanism for biologically-induced iodine emissions from sea-ice

A. Saiz-Lopez et al.

Title Page

Abstract	Introduction
Conclusions	References
Tables	Figures

◄   ►►

◄   ►

Back   Close

Full Screen / Esc

Printer-friendly Version

Interactive Discussion

von Glasow, R., Sander, R., Bott, A., and Crutzen, P. J.: Modelling halogen chemistry in the marine boundary layer 1, cloud-free MBL, J. Geophys. Res., 107, 4341, doi:10.1029/2001JD000942, 2002.

von Glasow, R. and Crutzen, P. J.: Tropospheric halogen chemistry, in: The Atmosphere, Treatise in Geochemistry, Elsevier-Pergamon, Oxford, UK, 2007.

Wang, F., Saiz-Lopez, A., Mahajan, A. S., Gómez Martín, J. C., Armstrong, D., Lemes, M., Hay, T., and Prados-Roman, C.: Enhanced production of oxidised mercury over the tropical Pacific Ocean: a key missing oxidation pathway, Atmos. Chem. Phys., 14, 1323–1335, doi:10.5194/acp-14-1323-2014, 2014.

Wayne, R. P.: Chemistry of Atmospheres, 3rd Edn., Oxford University Press, Oxford, 2000.

Weeks, W. F. and Ackley, S. F.: The growth, structure and properties of sea ice, in: The Geophysics of Sea Ice, edited by: Untersteiner, N., Plenum, New York, 9–164, 1986.

Weissenberger, J., Dieckmann, G., Gradinger, R., and Spindler, M.: Sea ice: a cast technique to examine and analyze brine pockets and channel structure, Limnol. Oceanogr., 37, 179–183, 1995.

Werner, I.: Seasonal dynamics, cryo-pelagic interactions and metabolic rates of Arctic pack-ice and under-ice fauna, a review, Polarforschung, 75, 1–19, 2006.

Zemmelink, H. J., Delille, B., Tison, J. L., Hintsa, E. J., Houghton, L., and Dacey, J. W. H.: CO_2 deposition over the multi-year ice of the western Weddell Sea, Geophys. Res. Lett., 33, L13606, doi:10.1029/2006GL026320, 2006.

A mechanism for biologically-induced iodine emissions from sea-ice

A. Saiz-Lopez et al.

Title Page

Abstract	Introduction
Conclusions	References
Tables	Figures

|◄　　　►|

◄　　　►

Back　　　Close

Full Screen / Esc

Printer-friendly Version

Interactive Discussion

Table 1. Diffusion timescale as a function of depth below sea-ice surface and diffusion coefficient D via the diffusion length equation: $L^2 = 4\mathrm{d}t$, where, L = length (cm) and t = time (s).

Depth below sea-ice surface (cm)	$D = 10^{-7}\,\mathrm{cm}^2\,\mathrm{s}^{-1}$	$D = 5 \times 10^{-5}\,\mathrm{cm}^2\,\mathrm{s}^{-1}$	$D = 1.3 \times 10^{-4}\,\mathrm{cm}^2\,\mathrm{s}^{-1}$
2.5	1/2 yr	9 h	2.4 h
5.0	2 yr	2 d	9.5 h
10	8 yr	6 d	1.6 d
20	32 yr	23 d	6.4 d
30	72 yr	52 d	14 d
40	127 yr	93 d	25 d
50	196 yr	145 d	40 d

Table 2. Summary of additional iodine production and loss processes.

Reaction	Rate Constant
I_2 + DOM → products	$k = 7 \times 10^{-3}\,s^{-1}$ (coastal water)[a], $k = 5 \times 10^{-5}\,s^{-1}$ (open ocean)[a]
$I_2 + I^- \leftrightarrow I_3^-$	$K = 698$ (at 25 °C)[b,c]
Abiotic Release	I_2 ($\sim 2 \times 10^7$ molecules cm^{-2} s^{-1}),
	HOI ($\sim 3.5 \times 10^8$ molecules cm^{-2} s^{-1})[d]
Biogenic Release	HOI (271 fmol HOI cell^{-1} h^{-1})[e],
	HOI ($\sim 1 \times 10^{10}$ molecules cm^{-2} s^{-1})[f]
Organic Iodine Production	$CH_2I_2 = 1 \times 10^6$ molecule cm^{-2} s^{-1},
	$CH_2IBr = 2 \times 10^9$ molecule cm^{-2} s^{-1},
	$CH_2ICl = 5 \times 10^7$ molecule cm^{-2} s^{-1}, and
	$CH_3I = 2 \times 10^8$ molecule cm^{-2} s^{-1} from open leads[g];
	dihalomethanes (3 pptv)[h]

[a] Truesdale et al. (1995).
[b] Palmer et al. (1984).
[c] O'Driscoll et al. (2008).
[d] Carpenter et al. (2013).
[e] Hill and Manley (2009).
[f] Sturges et al. (1997).
[g] Mahajan et al. (2010).
[h] Carpenter et al. (2005).
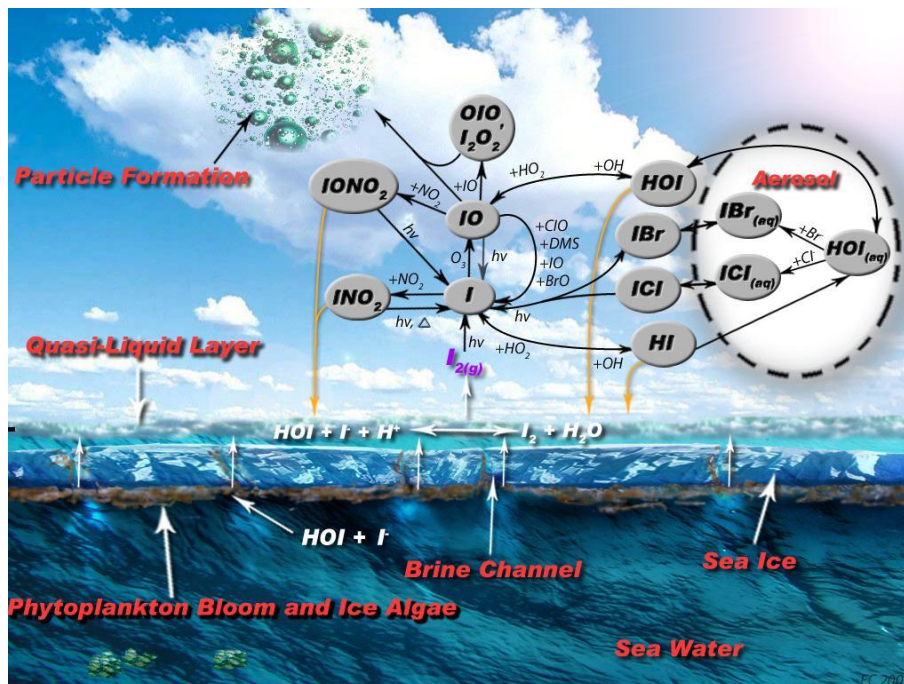
Figure 1. A simplified scheme of iodine cycling in and over Antarctic sea-ice. In and on the underside of Antarctic sea-ice the biological release of iodine into brine channels occurs. Subsequently diffusion of iodine through brine channels allows for the accumulation of these species in the QLL, releasing $I_{2(g)}$ to the atmosphere via gas phase equilibration. Thereafter transformations of compounds occur in the gas phase, and in deliquesced sea-salt aerosol.
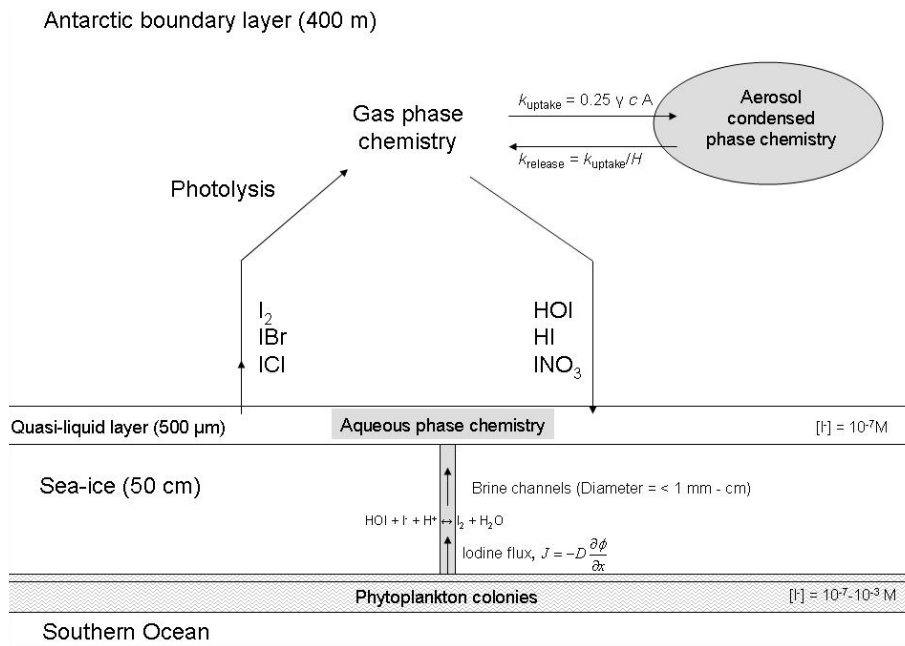
Figure 2. A simplified quantitative schematic of the proposed mechanism and the CON-AIR model structure. Note that the dimensions are not at real scale.
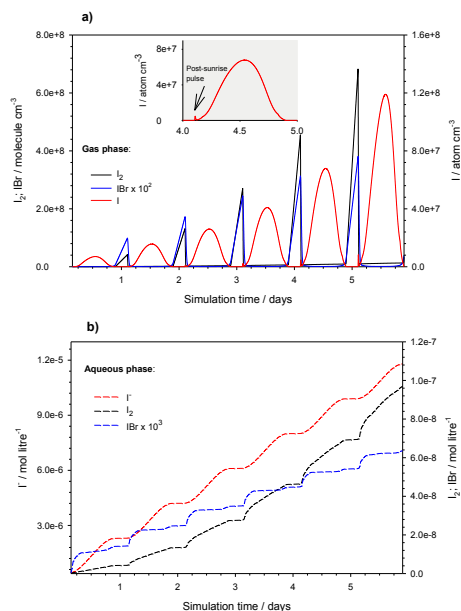
Figure 3. Iodine exchange from Antarctic sea-ice to the atmospheric boundary layer. **(a)** Gas phase I, I_2, and IBr. **(b)** Aqueous I^-, I_2, and IBr in the QLL. The post-sunrise pulse of I, shown in greater detail in the insert of Fig. 2a, is the result of the nighttime buildup of atmospheric I_2. Note that the emission of these species into the gas phase at night is slower than their production rates in the condensed phase. With time, the I^- concentration becomes comparable to that of Br^- and the reaction of HOI with I^-, to form I_2, competes with that of the acid with Br^-. The differences in the $I_{2(aq)}$ and $IBr_{(aq)}$ concentration profiles are due to the fact that the reverse rate constant to form $HOI + Br^-$, starting from $IBr_{(aq)}$, is orders of magnitude faster than that for formation of $HOI + I^-$, starting from $I_{2(aq)}$ (see Supplement). Note that this Figure corresponds to a diffusion timescale ~ 6 days ($D = 5 \times 10^{-5}\,cm^2\,s^{-1}$ at $\sim 10\,cm$ and $D = 1.3 \times 10^{-4}\,cm^2\,s^{-1}$ at $\sim 12.5\,cm$).
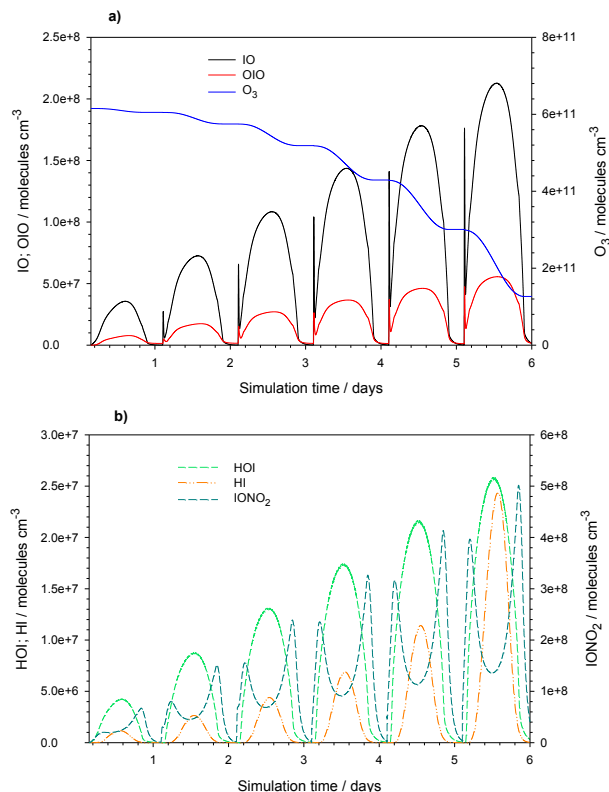
Figure 4. Modelled concentrations of gas phase iodine species resulting from the emission of I_2 from sea ice over six days from the start of the simulation. Following the buildup of I_2 during the preceding night, the model predicts a post-sunrise pulse of IO followed by a diurnal cycle shaped by solar radiation. The HOI (from $IO + HO_2$) and HI (from $I + HO_2$) profiles track the diurnal cycle of HO_2 and solar radiation. By contrast, $IONO_2$ will photolyze very efficiently during the day yielding its typical diurnal cycle with maxima in mid-morning and late afternoon.